JACS Au
AN OPEN ACCESS JOURNAL OF THE AMERICAN CHEMICAL SOCIETY

pubs.acs.org/jacsau
Article

Correlating Surface Chemistry to Surface Relaxivity via TD-NMR Studies of Polymer Particle Suspensions

Murilo T. Suekuni and Alan M. Allgeier*

Cite This: JACS Au 2023, 3, 2826−2834
Read Online

ABSTRACT: This study elucidates the impact of surface chemistry on solvent spin relaxation rates via time-domain nuclear magnetic resonance (TD-NMR). Suspensions of polymer particles of known surface chemistry were prepared in water and *n*-decane. Trends in solvent transverse relaxation rates demonstrated that surface polar functional groups induce stronger interactions with water with the opposite effect for *n*-decane. NMR surface relaxivities (ρ_2) calculated for the solid−fluid pairs ranged from 0.4 to 8.0 μm s^{-1} and 0.3 to 5.4 μm s^{-1} for water and *n*-decane, respectively. The values of ρ_2 for water displayed an inverse relationship to contact angle measurements on surfaces of similar composition, supporting the correlation of the TD-NMR output with polymer wettability. Surface composition, i.e., H/C ratios and heteroatom content, mainly contributed to the observed surface relaxivities compared to polymer % crystallinity and mean particle sizes via multiple linear regression. Ultimately, these findings emphasize the significance of surface chemistry in TD-NMR measurements and provide a quantitative foundation for future research involving TD-NMR investigations of wetted surface area and fluid-surface interactions. A comprehensive understanding of the factors influencing solvent relaxation in porous media can aid the optimization of industrial processes and the design of materials with enhanced performance.

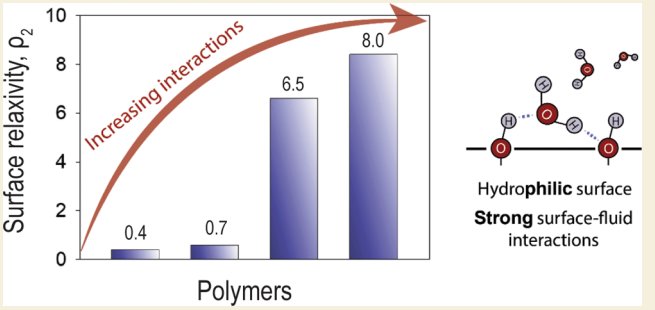

KEYWORDS: *TD-NMR, polymer science, surface−solvent interactions, adsorption energy, particle suspensions, surface relaxivity, solvent relaxation*

1. INTRODUCTION

Time-domain nuclear magnetic resonance (TD-NMR) is a convenient and nondestructive method to study porous media.[1] Compared to commonly used surface area characterization techniques, such as gas physisorption and mercury intrusion, it avoids time-consuming data collection and the structural damage of soft matter induced by aggressive outgassing or high-pressure analyses.[2,3] In TD-NMR studies, the enhanced relaxation rates of NMR-active nuclei, e.g., ^{1}H, characterize confinement effects and solid−fluid affinity of pore-entrapped molecules.[4,5] Although TD-NMR does not readily replace conventional techniques, characterizing pore fluid relaxation may allow scientists to rapidly characterize novel materials and study complex mass transport phenomena.[6,7]

In NMR analyses, the magnetic properties of specific atomic nuclei with nonzero spin prompt their parallel or antiparallel orientation with an externally applied magnetic field (B_0).[1] Upon reaching equilibrium, radiofrequency (RF) pulses, e.g., 90 or 180°, disrupt the acquired nuclei orientation. As B_0 is held constant, atomic re-equilibration occurs, characterized by specific time periods, namely, the spin−lattice (T_1) and spin−spin (T_2) relaxation times.[1,8] Compared to spectroscopy, which typically uses deuterated solvents and studies the chemical properties of the solute, time-domain, or solvent relaxation, experiments provide insights into fluid dynamics based on the solvent response.[5,9,10] Bulk liquids are highly mobile, and their relaxation times, usually on the order of seconds, are correlated with transport properties like self-diffusion coefficient and viscosity.[11] Inside porous media, fluid molecules will experience the influence of relaxation centers, e.g., paramagnetic or surface adsorption sites, resulting in reduced relaxation times.[4,12] In such systems, the surface relaxivity (ρ_i, i = 1 or 2) parameter can be determined experimentally and used as a criterion for the extent of solvent relaxation enhancement.[1] In paramagnetic-induced relaxation, electron−proton interactions dominate, and information on adsorption strength and material porosity is mostly limited.[13−15] In contrast, in the absence of paramagnetism, fluid relaxation rates may reflect dipolar couplings from inter- and intramolecular interactions of surface-adsorbed

Received: July 16, 2023
Revised: August 29, 2023
Accepted: September 19, 2023
Published: October 9, 2023

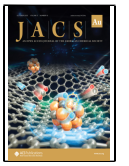

https://doi.org/10.1021/jacsau.3c00384
JACS Au 2023, 3, 2826−2834

molecules, and ρ_i may indicate solid−fluid interaction strength.[16] Surface chemistry is an important component in the design and performance of several industrially relevant processes, which can be optimized by leveraging the benefits of TD-NMR analyses.[17−19]

Substantial work has been done comprising TD-NMR studies of porous media, including particle suspensions,[20−23] catalysis,[24−27] zeolites[7,28,29] construction products,[30,31] and bioengineering.[32−36] Additionally, in the petroleum field, NMR logging allows the evaluation of the porosity and permeability of reservoir rocks and shales upon calibration via laboratory measurements.[37−40] The impact of surface chemistry on solvent relaxation measurements has been acknowledged in several studies. For instance, Schlumberger et al. showed that Stöber silicas may have a wetting preference for water compared to ethanol and tetrahydrofuran using T_1 and T_2 measurements.[21] The authors hypothesized that access to ultramicropores was limited by the kinetic diameter of the probe fluid, resulting in higher specific surface areas estimated from TD-NMR data of water-saturated samples compared to their ethanol counterparts and the argon physisorption benchmark.[21] Cosgrove et al. compared multiple silica samples and showed that without proper calibration, the differences in their surface composition, e.g., the density of silanol and siloxane groups, can lead to overestimated surface areas from T_2 data.[18] In tests with carbonaceous materials, Marchesini et al. correlated increased relaxation rates of protic and aprotic solvents to graphite surface heteroatom (O, N) content for samples modified via plasma functionalization.[41] Sharma et al. recently promoted solvent relaxation as an alternative method to estimate the Hansen solubility parameters for dispersions of carbon black samples.[22] It is clear that the solid−fluid interaction strength impacts solvent relaxation data. However, a molecular-level understanding of the influence of surface functional groups remains underexplored and limits the elaboration and predictive power of TD-NMR characterization techniques. This gap is surprising given its relevance to fundamental and practical studies and the significant body of work correlating the hydration numbers of molecules to system physicochemical properties.[42−46]

In this study, synthetic copolymers with varying well-defined surface chemistries were suspended in a polar (water) and a nonpolar (*n*-decane) solvent to elucidate qualitative and quantitative correlations between surface chemistry and NMR surface relaxivity. The insights enable progress toward the long-term goals of providing a molecular-level understanding of TD-NMR characterization techniques and allowing the prediction of surface relaxivity. The reported ρ_2 values help elucidate the importance of surface chemistry in TD-NMR methods and may serve as a reference for future studies of complex systems with similar chemical traits. It is notable that polymer particle suspensions are widely used in pharmaceuticals,[47] printing technologies,[48] composite manufacturing,[15,49] and coatings.[50] With such diverse applications, the systems under study serve not only as control samples but also represent commercial applications governed by fluid−surface interactions.

2. EXPERIMENTAL SECTION

2.1. Materials

Polystyrene (PS), poly(acrylic acid) (PAA), poly(ethylene-*co*-acrylic acid) (PE-AA), poly(4-vinylpyridine-*co*-styrene) (P4VP-S), poly(vinyl alcohol-*co*-ethylene) (PVOH-EE), poly(styrene-*co*-allyl alcohol) (PS-AAL), and Nylon-6 were purchased from Sigma-Aldrich. Table 1 provides the molar compositions of the tested copolymers, as provided by the supplier. Poly(ethylene terephthalate) (PET) was obtained from Goodfellow Materials. Kevlar pulp 1F538 was provided by DuPont Safety & Construction (Richmond, VA). ChromAR-grade water was purchased from Macron Fine Chemicals, and *n*-decane (≥99%) was obtained from Fisher Scientific.

Table 1. Molar Composition of Tested Copolymers as Reported by the Supplier

copolymer	molar composition (mol %)
poly(ethylene-*co*-acrylic acid)	95% ethylene, 5% acrylic acid
poly(4-vinylpyridine-*co*-styrene)	90% 4-vinylpyridine, 10% styrene
poly(vinyl alcohol-*co*-ethylene)	68% vinyl alcohol, 32% ethylene
poly(styrene-*co*-allyl alcohol)	60% styrene, 40% allyl alcohol

Figure 1 presents the chemical structures of the polymers studied here.

2.2. Particle Size Reduction

Fine polymer powders were obtained via cryogenic milling using an SPEX 6770 SamplePrep Freezer Mill. Approximately 2 g of polymer samples were loaded into polycarbonate vials and ground at liquid N_2 temperature (−196 °C). The milling procedure comprised 10 or 20 min of precooling, 4 cycles of 1 min grinding at 10 CPS (counts per second), and 1 min cool time between runs. Kevlar pulp 1F538 and poly(acrylic acid) were used without grinding.

2.3. Laser Diffraction

The particle size distributions of the copolymers were obtained via laser diffraction (LD) using a Beckman Coulter LS 13 320 Particle Size Analyzer. Approximately 0.5 g of each polymer was dispersed in 5 mL of sodium hexametaphosphate solution at 5 wt %. Deionized water was added until the total volume reached 45 mL. Before data collection, a background scan was carried out for pure deionized water. The particle size distributions are presented in Figure S1, and the average particle sizes (d_{50}) are compiled in Table S1.

2.4. N_2 Physisorption

The specific surface areas (SSA) were characterized using the Brunauer−Emmett−Teller (BET) method via N_2 physisorption in a Micromeritics ASAP2020 Surface Area and Porosity Analyzer.[51] The reported values were calculated from the P/P_0 range between 0.01 to 0.25. Polymer samples were degassed at 60 °C for 12 h at less than 5 μm Hg before data collection. The specific surface areas are presented in Table S1.

2.5. X-ray Diffraction

Powder X-ray diffraction (XRD) data were collected using a Bruker D2 Phaser Diffractometer with Co Kα (λ = 1.7890 Å), operated at 30 kV and 10 mA. Diffractograms were obtained at room temperature (295 K) with 2θ values ranging from 5 to 90° with a step size of 0.02° and rate of 0.3 s/step. For comparison with the literature, the XRD diffractograms were converted to 2θ values equivalent to those obtained using Cu Kα radiation (λ = 1.5406 Å). The %crystallinity (%C) values were estimated via curve fitting. See Supporting Information.[52]

2.6. Helium Pycnometry

The skeletal densities were determined via He pycnometry using a Micromeritics AccuPyc II 1340 Gas Pycnometer. The reported volumes and densities characterize the average value of 10 repeated cycles. The total uncertainty was propagated from the random and systematic uncertainties found from 10 different sample preparations and 7 consecutive polyethylene analyses. Most polymers were vacuum-dried at 60 °C for 12 h before data collection. Kevlar was vacuum-dried at 120 °C for 12 h. The skeletal densities are presented in Table S1.

2.7. Time-Domain Nuclear Magnetic Resonance (TD-NMR)

Transverse relaxation time data were collected using the Carr−Purcell−Meiboom−Gill pulse sequence using a Bruker Minispec mq-20 (0.47 T, 20 MHz) maintained at 20 °C using a Julabo CP-200F circulator bath.[53,54] Each magnetization decay curve comprised 30,000 echoes, collected with a 90−180° pulse time spacing (τ) of 0.2 ms and a recycle

https://doi.org/10.1021/jacsau.3c00384
JACS Au 2023, 3, 2826−2834

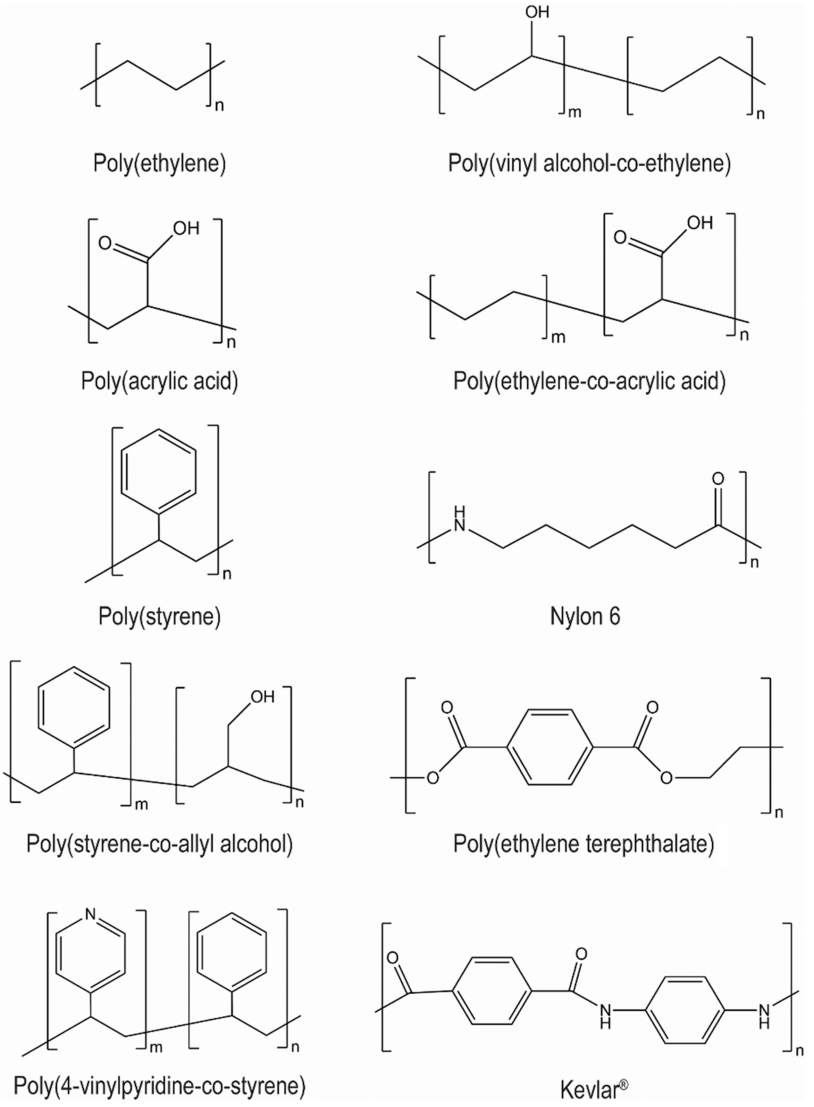

Figure 1. Chemical structures of the polymers used in this study.

delay of 4.5 s (*n*-decane) or 10 s (water). Particle suspensions with polymer concentrations varying from 1.3 to 10.0 wt % solid were prepared in 8 × 40 mm^2 glass vials. Homogeneous dispersion was promoted by vigorous stirring using an IKA Minishaker. Samples were vacuum-dried (<77 Torr) at 60 °C for 12 h using a VWR Vacuum Oven before suspension in liquids. Measurements were performed in triplicate.

The observed solvent transverse relaxation rates were assessed based on their correlation to the surface chemistry and system porosity, eq 1.

$$\frac{1}{T_2} = \frac{1}{T_{2b}} + \rho_2 \frac{S}{V} \quad (1)$$

T_{2b} represents the transverse relaxation time of the bulk fluid (2.3 s for water and 1.3 s for *n*-decane at 20 °C), ρ_2 represents the transverse surface relaxivity, S the total particle surface area interacting with the fluid, and V the fluid volume. The values of T_{2b} were determined separately for the pure liquid samples. Effects of relaxation induced by molecular diffusion and magnetic field gradient in the observed T_2 are eliminated by the use of low-intensity magnetic fields and short echo-spacing separation.[38,55,56] Because of their hindered translational motion, solids possess small T_2 values, in the order of μs, and are undetectable in the tested conditions.[57] The uncertainties in T_2 and ρ_2 were assessed based on the random and systematic uncertainties in sample preparation, the relaxation time of the bulk fluid, and the specific surface area of the polymers, see Supporting Information.

2.8. Interparticle Spacing Calculations

Interparticle spacing (IPS) calculations were performed using the model proposed by Hao and Riman, assuming homogeneous dispersion of spherical particles surrounded by a liquid cell, eq 2.[58]

$$\mathrm{IPS} = 2r_{\mathrm{Pol}}\left[\left(\frac{\phi_m}{\phi}\right)^{1/3} - 1\right] \quad (2)$$

where r_{Pol} represents the polymer particle radius, estimated using laser diffraction analysis; ϕ the polymer volume fraction; and ϕ_m the maximum packing fraction density, taken as 0.59 for random loose packing.[58] Here, ϕ was determined based on the polymer and liquid masses and the densities obtained from He pycnometry (Table S1).

3. RESULTS AND DISCUSSION

3.1. Characterization of Polymer Wettability via TD-NMR

Solvent relaxometry is a convenient analytical method for porous media and particle suspensions as it allows sample characterization under their conditions of use.[18,59] In TD-NMR experiments, the observed solvent relaxation rates provide insights into the material wetted surface area and solid−fluid affinity. Intermolecular interactions may induce faster relaxation of surface-adsorbed molecules compared to their "undisturbed"

https://doi.org/10.1021/jacsau.3c00384
JACS Au 2023, 3, 2826−2834

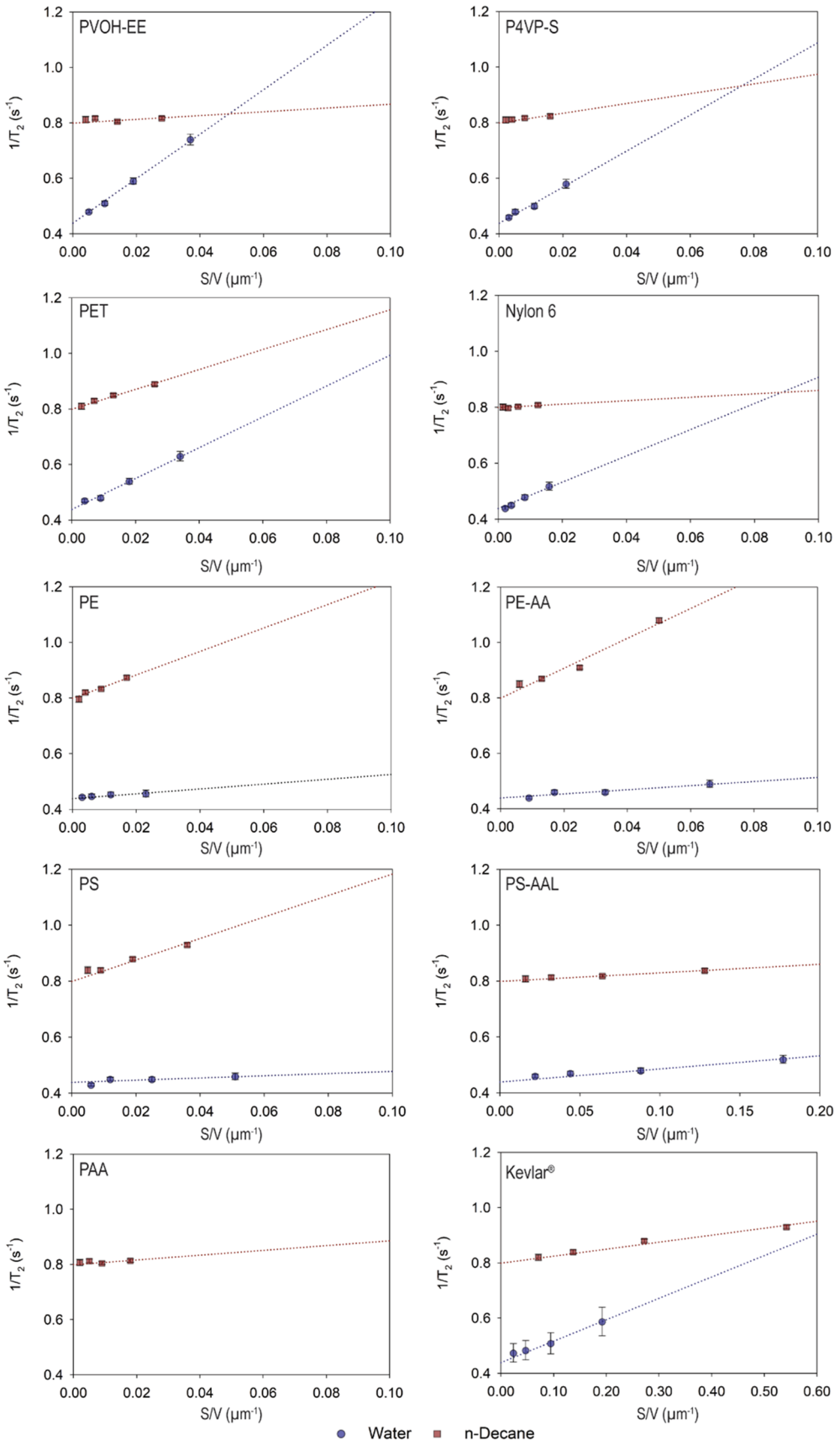

Figure 2. $1/T_2$ data for polymer particle suspensions.

state.[12] In particle suspensions, the observed T_2 will depend on the frequency and strength of surface-fluid interactions as a reflection of the relative populations of surface-bound and free fluid molecules.[60] Accordingly, the solid concentration and $1/T_2$

https://doi.org/10.1021/jacsau.3c00384
JACS Au 2023, 3, 2826−2834

are expected to be positively correlated. Following these principles, Figure 2 displays the transverse relaxation rate data of the tested polymer particle suspensions in water and *n*-decane versus the respective surface-to-volume ratios. The data for PAA in water are not shown because it dissolved at the tested conditions; see Figures S3 and S4. The data for Kevlar in water are taken from Suekuni et al.[15] The intercepts were set as the $1/T_{2b}$ of deionized water (0.44 s^{-1}) and *n*-decane (0.80 s^{-1}) at 20 °C. The plotted error bars represent a rigorous uncertainty assessment within a 95% confidence interval, see Supporting Information.

Traditionally, materials are identified by whether they get wet by (philic) or repel (phobic) liquids, with water (hydrophilic/hydrophobic) and hydrocarbons (oleophilic/oleophobic) as common probing fluids.[61] This fluid−surface compatibility is generally explained by fundamental concepts such as the "like-dissolve-like" rule, where polar moieties are expected to facilitate interactions with polar liquids.[62] The trends in $1/T_2$ were notably regulated by polymer surface chemistry with a general opposite behavior for water and *n*-decane for most of the tested samples. Accordingly, the slopes of polymers with a high affinity for water were steeper than their response to *n*-decane and vice versa. Certain functional groups can induce preferential attraction or repulsion of fluids, regulating the wetting properties of surfaces. Figure 3 presents the transverse surface relaxivities

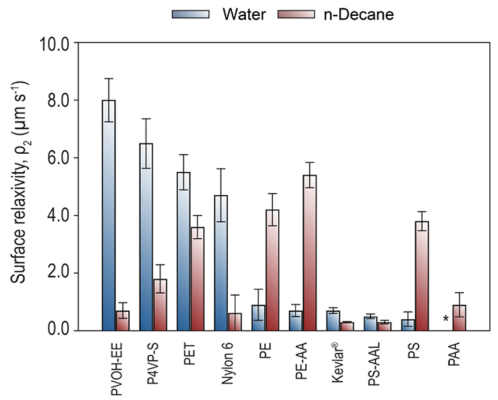

Figure 3. Transverse surface relaxivities of polymer−water and polymer-decane pairs. Kevlar (water) was obtained from Suekuni et al.[15]

linearly regressed by using eq 1 ordered by the observed affinity to water. Here, bar charts are used to clarify the trends and help elucidate their correlation to the expected wetting nature of the tested polymers. The reported values were regressed under the assumption that relaxation occurred in the fast-diffusion regime limit, where surface-bound and bulk fluid molecules are assumed to be diffusionally averaged throughout the experimental time.[38,63] Here, a dimensionless parameter (k) was used to assess the validity of this assumption, as shown in eq 3.

$$k = \frac{\rho_2 \alpha}{D} \tag{3}$$

where α represents half of the interparticle spacing (see Section 2) and D is the liquid self-diffusion coefficient. At 20 °C, $D_{water} \sim 2.0 \times 10^{-5}$ cm^2 s^{-1} and $D_{decane} \sim 1.4 \times 10^{-5}$ cm^2 s^{-1}.[64,65] Based on the theory, systems with $k \ll 1.0$ correspond to the fast-diffusion regime limit and the observed relaxation rates are directly associated with the pore surface chemistry and surface-to-volume ratio.[38,63,66] In this study, k (water or *n*-decane) < 0.05, validating the assumption that the fast-diffusion regime criterion was met, Table S6. These values were calculated from the most diluted conditions tested, i.e., ∼1.3 wt % polymer, representing the largest interparticle spacing in suspension.

PVOH-EE and P4VP-S yielded the highest surface relaxivities for water of the tested sample set, reflecting their mostly polar compositions (Table 1). Notably, the regressed ρ_2 values for *n*-decane of these polymers are 4−11 times lower, indicating the preference for interactions with polar liquids. The regressed ρ_2 values for Nylon-6 and PET were slightly lower than those of the first two copolymers. Such values can be associated with the contributions from the oxygen- and nitrogen-bearing moieties. Ono and Shikata showed that amide groups present high hydration numbers, i.e., 5−6 water molecules per group, supporting the high surface relaxivity of Nylon.[67] Additionally, this value is in good quantitative agreement with the study by Fieremans et al., who reported a ρ_2 of 4.6 μm s^{-1} for Nylon-6,12.[68] For the case of PET, although ester groups have been recently classified as hydroneutral in dielectric relaxation studies, they can serve as H-bond acceptors in interactions with water and possess a similar dipole moment compared with the hydroxyl group.[44] Furthermore, previous studies have shown that PET possesses a hygroscopic behavior, absorbing moisture from its surroundings.[69] PET is the only polymer tested with a high surface relaxivity for both liquids, suggesting an amphiphilic behavior with a slight preference for water.

PE and PS, which are traditionally known for their hydrophobic nature, displayed $\rho_2 < 1.0$ μm s^{-1}, in good quantitative agreement with previous work. Fieremans et al. reported a ρ_2 of 0.1 μm s^{-1} for ultrahigh molecular weight PE in water and Hansen et al., a ρ_2 of 0.4 μm s^{-1} for poly(styrene) beads cross-linked with divinylbenzene.[68,70] The relatively small concentration of acrylic acid of PE-AA did not result in a higher affinity for water, and its ρ_2 is similar to PE. In fact, their (PE, PE-AA) response to *n*-decane is almost the same within the estimated uncertainty. Besides, the ρ_2 values of PE and PE-AA for *n*-decane are larger than the one regressed for PS, reflecting the preferred interactions with alkane chains and the contributions of the higher proton density at the surface, favoring intermolecular proton−proton relaxation. Kevlar is known for its rigid polymeric structure, reflecting the low mobility of phenyl rings and the strong intermolecular hydrogen bonding between amide groups.[71] These characteristics grant Kevlar its high tensile strength and low solubility, which might reflect the low surface relaxivities observed here.[72] Surprisingly, PS-AAL also showed low surface relaxivity values for both liquids. Jeong et al. recently discussed the dominance of dispersive over polar forces in PS-AAL (40% AAL) surfaces, reporting contact angles of ∼73 and ∼32° for water and diiodomethane, respectively.[73] These values agree with the past studies by Lee et al., who reported values of ∼81° (water) and ∼30° (diiodomethane) for PS-AAL (5.4−6.0% AAL).[74] Comparison of these two works suggests that the allyl alcohol concentration does not significantly enhance the water wettability of PS-AAL regardless of the noticeable difference in the alcohol content. The dominance of dispersive surface forces, as reported in both studies, may contribute to the observed water-repelling nature of PS-AAL and the similar ρ_2 of PS-AAL (0.5 ± 0.1 μm s^{-1}) and PS (0.4 ± 0.2 μm s^{-1}) for water. However, the low ρ_2 of PS-AAL for *n*-decane requires further investigation.

https://doi.org/10.1021/jacsau.3c00384
JACS Au 2023, 3, 2826−2834

3.2. Comparison of ρ_2 and Water Contact Angles

The results of other surface-sensitive methods can help qualitatively assess the observed trends. Hence, ρ_2 was compared with water contact angles (WCA) on polymers of equivalent composition from the literature, Figure 4.[73,75−80]

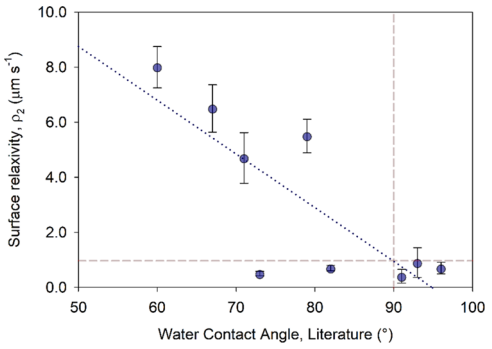

Figure 4. Comparison of the regressed surface relaxivities with contact angle measurements of equivalent polymers from the literature.

Here, two red dashed lines were used to mark the contact angle of 90°, traditionally known as the limit between hydrophilic and hydrophobic materials and $\rho_2 = 1.0\ \mu m\ s^{-1}$. The comparison was restricted to water because finite contact angles for low surface tension liquids, such as normal alkanes, are rarely achievable under atmospheric conditions and require special features, e.g., fluorination and engineered topography.[81,82] Further information about the contact angles used is provided in Table S4.

A general inverse relationship between ρ_2 and water contact angles was observed, supporting the relationship between the polymer hydrophilicity and the surface relaxivity value for water. A linear regression, represented by the dotted blue line, showed a $R^2 = 0.64$. Remarkably, the absence or the negligible heteroatom content contributed to a subpopulation of hydrophobic polymers by both techniques, i.e., PE, PE-AA, and PS, suggesting a useful correlation for practical applications. Kevlar and PS-AAL were outliers in the trend, with $\rho_2 < 1.0\ \mu m\ s^{-1}$ and WCA < 90°. The influence of several aspects that may contribute to polymer ρ_2 is evaluated in the following section.

3.3. Evaluating Contributing Factors to ρ_2

A quantitative assessment of contributing factors to polymer surface relaxivity was implemented through multiple linear regression analysis, considering the unique contributions of predictor variables (x_j) and their respective slopes (β_j), eq 4.[83]

$$Y = \beta_0 + \sum \beta_j x_j \tag{4}$$

where Y and β_0 are the mean dependent variables and the regressed intercept, respectively. Here, the heteroatom content (h_c), the hydrogen-to-carbon ratios (H/C), the %C, and d_{50} of the copolymers were considered predictors of ρ_2. The value of h_c was taken as the oxygen-to-carbon ratio for all polymers except P4VP, where the nitrogen-to-carbon ratio was used, calculated based on the molar compositions from Table 1, along with H/C ratios. The multiple linear regression analyses were conducted using the Minitab Statistical Software.

From the calculations, the polymer chemical composition (h_c and H/C) was the most relevant predictor for ρ_2 toward water and *n*-decane, with values 2−3 orders of magnitude greater than %C and d_{50}, eqs 5 and 6. The *p*-values of each contributor are presented in Table S7. For the current data set, only h_c (water) showed a *p*-value ≤ 0.05. No interactions between variables were observed for the considered predictors. Future studies that expand this database may support more statistically significant values.

$$\rho_{2,water} = -1.170 + 18.000(h_c) + 1.670(H/C) - 0.018(\%C) - 0.002(d_{50}) \tag{5}$$

$$\rho_{2,decane} = 2.400 - 3.710(h_c) + 0.610(H/C) - 0.009(\%C) - 0.001(d_{50}) \tag{6}$$

As expected, while h_c has a positive relationship with $\rho_{2,water}$, it has the opposite behavior for $\rho_{2,decane}$, in agreement with the "like-dissolve-like rule." The hydrogen-to-carbon ratios showed positive correlations in both cases. However, the concentration of heteroatoms played a more significant role, indicating that hydrogen bonding has a stronger effect on solvent relaxation than homonuclear dipolar coupling. The correlation to heteroatom content may not capture the diverse properties of moieties, considering, for example, the different hydration numbers of oxygen- and nitrogen-bearing groups.[43,44] Further investigation comparing such characteristics may yield more accurate predictors of ρ_2 from the polymer composition and physical attributes. Highly crystalline polymers possess low surface free energy and are more resistant to surface treatments compared to their amorphous counterparts, given the strong intermolecular bonding between the chains.[84,85] However, polymer crystallinity only weakly reduced the surface relaxivities, showing that surface chemistry is the most important contributor. These results agree with water wettability studies by Borcia et al., who did not observe strong correlations between the wettability and crystallinity of a series of polymers.[86] The equally weak correlation to the average particle size indicates that small particles of high surface areas did not bias the observed values.

4. CONCLUSIONS

Time-domain NMR is a convenient and noninvasive method to study porous media under in situ conditions. Herein, trends in the transverse relaxation rates of polymer particles suspended in water and *n*-decane were used to probe the impact of surface chemistry upon solvent relaxation. The regressed ρ_2 for polymer−water and polymer-*n*-decane pairs reflected their expected chemical affinity, ranging from 0.4 to 8.0 $\mu m\ s^{-1}$ (water) and 0.3 to 5.4 $\mu m\ s^{-1}$ (*n*-decane). The correlation between ρ_2 and the polymer wetting properties was further supported by comparison with the water contact angle data from the literature. Polymer heteroatom (O, N) content, H/C ratios, %crystallinity, and average particle sizes were considered as predictor variables for ρ_2 in multiple linear regression analyses. The obtained trends showed that surface chemistry (h_c and H/C) has a superior influence upon ρ_2 compared with crystallinity and particle size, with the content of heteroatoms as the most influential. Kevlar and PS-AAL were outliers in the assessed trends and may be the objectives of future investigations. Developing a database of surface relaxivities is important to decouple the effects from composition to material porosity, supporting the development and accuracy of TD-NMR methods. Furthermore, well-defined surface chemistries may provide a benchmark for understanding fluid relaxation in pores of naturally occurring materials.

https://doi.org/10.1021/jacsau.3c00384
JACS Au 2023, 3, 2826−2834

■ ASSOCIATED CONTENT

Supporting Information

The Supporting Information is available free of charge at https://pubs.acs.org/doi/10.1021/jacsau.3c00384.

Polymer particle size distributions, specific surface areas, skeletal densities, uncertainty assessment for T_2 and ρ_2, X-ray diffraction data, polymer solubility assessment, and regressed contributors and *p*-values (PDF)

■ AUTHOR INFORMATION

Corresponding Author

Alan M. Allgeier − *Department of Chemical and Petroleum Engineering, The Center for Environmentally Beneficial Catalysis, and The Institute for Sustainable Engineering, University of Kansas, Lawrence, Kansas 66045, United States;* orcid.org/0000-0001-9122-2108; Email: alan.allgeier.ku.edu

Author

Murilo T. Suekuni − *Department of Chemical and Petroleum Engineering, The Center for Environmentally Beneficial Catalysis, and The Institute for Sustainable Engineering, University of Kansas, Lawrence, Kansas 66045, United States;* orcid.org/0000-0003-1558-6780

Complete contact information is available at: https://pubs.acs.org/10.1021/jacsau.3c00384

Notes

The authors declare no competing financial interest.

■ ACKNOWLEDGMENTS

The authors acknowledge the financial support from the American Chemical Society-Petroleum Research Funds (ACS-PRF) grant (61103-ND10); DuPont Safety and Construction for the generous donation of the Kevlar sample; and Spencer Kiessling from the Kansas Geological Survey for his assistance with the laser diffraction analysis.

■ REFERENCES

(1) Kinn, B. E.; Myers, T. R.; Allgeier, A. M. Surface Enhanced Nuclear Magnetic Resonance Relaxation Mechanisms and Their Significance in Chemical Engineering Applications. *Curr. Opin. Chem. Eng.* **2019**, *24*, 115−121.

(2) Suekuni, M. T.; Craddock, P. R.; Douglas, J. T.; Pomerantz, A. E.; Allgeier, A. M. Critical Practices for the Preparation and Analysis of Kerogen. *Energy Fuels* **2022**, *36* (16), 8828−8843.

(3) Wang, X.; Peng, Y.; Wang, J.; Zeng, Q. Pore Structure Damages in Cement-Based Materials by Mercury Intrusion: A Non-Destructive Assessment by X-Ray Computed Tomography. *Materials* **2019**, *12* (14), 2220.

(4) D'Agostino, C.; Mitchell, J.; Mantle, M. D.; Gladden, L. F. Interpretation of NMR Relaxation as a Tool for Characterising the Adsorption Strength of Liquids inside Porous Materials. *Chem. − Eur. J.* **2014**, *20* (40), 13009−13015.

(5) Chen, J. J.; Kong, X.; Sumida, K.; Manumpil, M. A.; Long, J. R.; Reimer, J. A. Ex Situ NMR Relaxometry of Metal-Organic Frameworks for Rapid Surface-Area Screening. *Angew. Chem., Int. Ed.* **2013**, *52* (46), 12043−12046.

(6) Chen, J. J.; Mason, J. A.; Bloch, E. D.; Gygi, D.; Long, J. R.; Reimer, J. A. NMR Relaxation and Exchange in Metal−Organic Frameworks for Surface Area Screening. *Microporous Mesoporous Mater.* **2015**, *205*, 65−69.

(7) Marreiros, J.; de Oliveira-Silva, R.; Iacomi, P.; Llewellyn, P. L.; Ameloot, R.; Sakellariou, D. Benchtop *In Situ* Measurement of Full Adsorption Isotherms by NMR. *J. Am. Chem. Soc.* **2021**, *143* (22), 8249−8254.

(8) Thomson, C. E.; Kornegay, J. N.; Burn, R. A.; Drayer, B. P.; Hadley, D. M.; Levesque, D. C.; Gainsburg, L. A.; Lane, S. B.; Sharp, N. J. H.; Wheeler, S. J. Magnetic Resonance Imaging - A General Overview of Principles and Examples in Veterinary Neurodiagnosis. *Vet. Radiol. Ultrasound* **1993**, *34* (1), 2−17.

(9) Korb, J.-P. Nuclear Magnetic Relaxation of Liquids in Porous Media. *New J. Phys.* **2011**, *13* (3), No. 035016.

(10) Maillet, B.; Sidi-Boulenouar, R.; Coussot, P. Dynamic NMR Relaxometry as a Simple Tool for Measuring Liquid Transfers and Characterizing Surface and Structure Evolution in Porous Media. *Langmuir* **2022**, *38* (49), 15009−15025.

(11) Bloembergen, N.; Purcell, E. M.; Pound, R. V. Relaxation Effects in Nuclear Magnetic Resonance Absorption. *Phys. Rev.* **1948**, *73* (7), 679−712.

(12) Pfeifer, H. Nuclear Magnetic Resonance and Relaxation of Molecules Adsorbed on Solids. In *NMR Basic Principles and Progress*; Diehl, P.; Fluck, E.; Kosfeld, R., Eds.; Springer: Berlin, 1972; pp 53−153.

(13) Keating, K.; Knight, R. The Effect of Spatial Variation in Surface Relaxivity on Nuclear Magnetic Resonance Relaxation Rates. *Geophysics* **2012**, *77* (5), E365−E377.

(14) Foley, I.; Farooqui, S. A.; Kleinberg, R. L. Effect of Paramagnetic Ions on NMR Relaxation of Fluids at Solid Surfaces. *J. Magn. Reson., Ser. A* **1996**, *123* (1), 95−104.

(15) Suekuni, M. T.; Myers, T. R.; McNeil, M. C.; Prisco, A. J.; Shelburne, S. S.; Shepperson, W. A.; Allgeier, A. M. Surface Area Determination of Kevlar Particles in Suspensions Containing Iron Impurities Using Low-Field Nuclear Magnetic Resonance Relaxometry. *ACS Appl. Polym. Mater.* **2020**, *2* (6), 2134−2141.

(16) Robinson, N.; Robertson, C.; Gladden, L. F.; Jenkins, S. J.; D'Agostino, C. Direct Correlation between Adsorption Energetics and Nuclear Spin Relaxation in a Liquid-Saturated Catalyst Material. *ChemPhysChem* **2018**, *19* (19), 2472−2479.

(17) Somorjai, G. A.; Li, Y. Impact of Surface Chemistry. *Proc. Natl. Acad. Sci. U.S.A.* **2011**, *108* (3), 917−924.

(18) Cosgrove, T.; Stebbing, S.; Ackroyd, M.; Fairhurst, D.; Sanderson, K.; Prescott, S. W. Using Low-Field NMR Relaxation to Optimise Particulate Dispersions. *Powder Technol.* **2023**, *414*, No. 118065.

(19) Marchesini, S.; Turner, P.; Paton, K. R.; Reed, B. P.; Pollard, A. J. Rapid Monitoring of Graphene Exfoliation Using NMR Proton Relaxation. *Nanoscale* **2021**, *13* (34), 14518−14524.

(20) Silletta, E. V.; Velasco, M. I.; Gomez, C. G.; Strumia, M. C.; Stapf, S.; Mattea, C.; Monti, G. A.; Acosta, R. H. Enhanced Surface Interaction of Water Confined in Hierarchical Porous Polymers Induced by Hydrogen Bonding. *Langmuir* **2016**, *32* (29), 7427−7434.

(21) Schlumberger, C.; Sandner, L.; Michalowski, A.; Thommes, M. Reliable Surface Area Assessment of Wet and Dry Nonporous and Nanoporous Particles: Nuclear Magnetic Resonance Relaxometry and Gas Physisorption. *Langmuir* **2023**, *39* (13), 4611−4621.

(22) Sharma, R.; Fairhurst, D.; Growney, D. J.; Dümpelmann, R.; Cosgrove, T. Using NMR Solvent Relaxation to Determine the Hansen Solubility Parameters of a Carbon Black and as a Quick Method to Compare the Surface Quality of Carbon Blacks. *Colloid Polym. Sci.* **2023**, *301*, 851−861.

(23) Elliott, L. N.; Austin, D.; Bourne, R. A.; Hassanpour, A.; Robb, J.; Edwards, J. L.; Sutcliffe, S.; Hunter, T. N. Analysis of Adsorbed Polyphosphate Changes on Milled Titanium Dioxide, Using Low-Field Relaxation NMR and Photoelectron Spectroscopy. *Langmuir* **2023**, *39* (16), 5697−5709.

(24) Mitchell, J.; Broche, L. M.; Chandrasekera, T. C.; Lurie, D. J.; Gladden, L. F. Exploring Surface Interactions in Catalysts Using Low-Field Nuclear Magnetic Resonance. *J. Phys. Chem. C* **2013**, *117* (34), 17699−17706.

(25) Krzyżak, A.; Habina, I. Low Field 1 H NMR Characterization of Mesoporous Silica MCM-41 and SBA-15 Filled with Different Amount of Water. *Microporous Mesoporous Mater.* **2016**, *231*, 230−239.
(26) Robinson, N.; May, E. F.; Johns, M. L. Low-Field Functional Group Resolved Nuclear Spin Relaxation in Mesoporous Silica. *ACS Appl. Mater. Interfaces* **2021**, *13* (45), 54476−54485.
(27) D'Agostino, C.; Armstrong, R. D.; Hutchings, G. J.; Gladden, L. F. Product Inhibition in Glycerol Oxidation over Au/TiO_2 Catalysts Quantified by NMR Relaxation. *ACS Catal.* **2018**, *8* (8), 7334−7339.
(28) D'Agostino, C.; Bräuer, P.; Zheng, J.; Robinson, N.; York, A. P. E.; Song, L.; Fan, X. Adsorbate/Adsorbent Interactions in Microporous Zeolites: Mechanistic Insights from NMR Relaxation and DFT Calculations. *Mater. Today Chem.* **2023**, *29*, No. 101443.
(29) Robinson, N.; Bräuer, P.; York, A. P. E.; D'Agostino, C. Nuclear Spin Relaxation as a Probe of Zeolite Acidity: A Combined NMR and TPD Investigation of Pyridine in HZSM-5. *Phys. Chem. Chem. Phys.* **2021**, *23* (33), 17752−17760.
(30) Dalas, F.; Korb, J.-P.; Pourchet, S.; Nonat, A.; Rinaldi, D.; Mosquet, M. Surface Relaxivity of Cement Hydrates. *J. Phys. Chem. C* **2014**, *118* (16), 8387−8396.
(31) Robinson, N.; Nasharuddin, R.; Fridjonsson, E. O.; Johns, M. L. NMR Surface Relaxivity in a Time-Dependent Porous System. *Phys. Rev. Lett.* **2023**, *130* (12), No. 126204.
(32) Wang, X.; Ni, Q. Determination of Cortical Bone Porosity and Pore Size Distribution Using a Low Field Pulsed NMR Approach. *J. Orthop. Res.* **2003**, *21* (2), 312−319.
(33) Fraenza, C. C.; Meledandri, C. J.; Anoardo, E.; Brougham, D. F. The Effect of Cholesterol on Membrane Dynamics on Different Timescales in Lipid Bilayers from Fast Field-Cycling NMR Relaxometry Studies of Unilamellar Vesicles. *ChemPhysChem* **2014**, *15* (3), 425−435.
(34) Suekuni, M. T.; D'Souza, N.; Allgeier, A. M. NMR Relaxometry Studies on the Drying Kinetics of Cellulose Nanofibers. *Ind. Eng. Chem. Res.* **2022**, *61* (16), 5475−5483.
(35) Kopač, T.; Abrami, M.; Grassi, M.; Ručigaj, A.; Krajnc, M. Polysaccharide-Based Hydrogels Crosslink Density Equation: A Rheological and LF-NMR Study of Polymer-Polymer Interactions. *Carbohydr. Polym.* **2022**, *277*, No. 118895.
(36) Burkey, K.; Castillo, K.; Elrod, P.; Suekuni, M. T.; Aikman, E.; Gehrke, S.; Allgeier, A.; Robinson, J. L. Modulating Pentenoate-functionalized Hyaluronic Acid Hydrogel Network Properties for Meniscal Fibrochondrocyte Mechanotransduction. *J. Biomed. Mater. Res.* **2023**, *111* (6), 1525−1537.
(37) Coates, G. R. Summary of NMR Logging Applications and Benefits. In *NMR Logging: Principles of Applications*; Haliburton Energy Services: Houston, TX, 1999; Vol. *234*, Chapter 1, pp 1−32.
(38) Washburn, K. E. Relaxation Mechanisms and Shales. *Concepts Magn. Reson.* **2014**, *43A* (3), 57−78.
(39) Panattoni, F.; Colbourne, A. A.; Fordham, E. J.; Mitchell, J.; Grey, C. P.; Magusin, P. C. M. M. Improved Description of Organic Matter in Shales by Enhanced Solid Fraction Detection with Low-Field ^{1}H NMR Relaxometry. *Energy Fuels* **2021**, *35* (22), 18194−18209.
(40) Godefroy, S.; Fleury, M.; Deflandre, F.; Korb, J.-P. Temperature Effect on NMR Surface Relaxation in Rocks for Well Logging Applications. *J. Phys. Chem. B* **2002**, *106* (43), 11183−11190.
(41) Marchesini, S.; Paton, K. R.; Brennan, B.; Turner, P.; Pollard, A. J. Using Nuclear Magnetic Resonance Proton Relaxation to Probe the Surface Chemistry of Carbon 2D Materials. *Nanoscale* **2021**, *13* (13), 6389−6393.
(42) Ono, Y.; Shikata, T. Hydration and Dynamic Behavior of Poly(*N*-Isopropylacrylamide)s in Aqueous Solution: A Sharp Phase Transition at the Lower Critical Solution Temperature. *J. Am. Chem. Soc.* **2006**, *128* (31), 10030−10031.
(43) Shikata, T.; Okuzono, M. Are All Polar Molecules Hydrophilic? Hydration Numbers of Ketones and Esters in Aqueous Solution. *J. Phys. Chem. B* **2013**, *117* (25), 7718−7723.
(44) Sagawa, N.; Shikata, T. Are All Polar Molecules Hydrophilic? Hydration Numbers of Nitro Compounds and Nitriles in Aqueous Solution. *Phys. Chem. Chem. Phys.* **2014**, *16* (26), 13262−13270.
(45) Satokawa, Y.; Shikata, T. Hydration Structure and Dynamic Behavior of Poly(Vinyl Alcohol)s in Aqueous Solution. *Macromolecules* **2008**, *41* (8), 2908−2913.
(46) Davis, J. G.; Gierszal, K. P.; Wang, P.; Ben-Amotz, D. Water Structural Transformation at Molecular Hydrophobic Interfaces. *Nature* **2012**, *491* (7425), 582−585.
(47) Lee, C. H.; Moturi, V.; Lee, Y. Thixotropic Property in Pharmaceutical Formulations. *J. Controlled Release* **2009**, *136* (2), 88−98.
(48) Tekin, E.; Smith, P. J.; Schubert, U. S. Inkjet Printing as a Deposition and Patterning Tool for Polymers and Inorganic Particles. *Soft Matter* **2008**, *4* (4), 703−713.
(49) Naskar, A. K.; Keum, J. K.; Boeman, R. G. Polymer Matrix Nanocomposites for Automotive Structural Components. *Nat. Nanotechnol.* **2016**, *11* (12), 1026−1030.
(50) De Riccardis, M. F.; Martina, V.; Carbone, D. Study of Polymer Particles Suspensions for Electrophoretic Deposition. *J. Phys. Chem. B* **2013**, *117* (6), 1592−1599.
(51) Brunauer, S.; Emmett, P. H.; Teller, E. Adsorption of Gases in Multimolecular Layers. *J. Am. Chem. Soc.* **1938**, *60* (2), 309−319.
(52) Murthy, N. S.; Minor, H. General Procedure for Evaluating Amorphous Scattering and Crystallinity from X-Ray Diffraction Scans of Semicrystalline Polymers. *Polymer* **1990**, *31* (6), 996−1002.
(53) Carr, H. Y.; Purcell, E. M. Effects of Diffusion on Free Precession in Nuclear Magnetic Resonance Experiments. *Phys. Rev.* **1954**, *94* (3), 630−638.
(54) Meiboom, S.; Gill, D. Modified Spin-Echo Method for Measuring Nuclear Relaxation Times. *Rev. Sci. Instrum.* **1958**, *29* (8), 688−691.
(55) Coates, G. R. Fundamentals of NMR Petrophysics. In *NMR Logging: Principles of Applications*; Haliburton Energy Services: Houston, TX, 1999; Vol. *234*, Chapter 3, pp 45−76.
(56) Stingaciu, L. R.; Pohlmeier, A.; Blümler, P.; Weihermüller, L.; Van Dusschoten, D.; Stapf, S.; Vereecken, H. Characterization of Unsaturated Porous Media by High-Field and Low-Field NMR Relaxometry. *Water Resour. Res.* **2009**, *45*, No. W08412.
(57) Litvinov, V.; Men, Y. Time-Domain NMR in Polyolefin Research. *Polymer* **2022**, *256*, No. 125205.
(58) Hao, T.; Riman, R. E. Calculation of Interparticle Spacing in Colloidal Systems. *J. Colloid Interface Sci.* **2006**, *297* (1), 374−377.
(59) Yuan, L.; Chen, L.; Chen, X.; Liu, R.; Ge, G. *In Situ* Measurement of Surface Functional Groups on Silica Nanoparticles Using Solvent Relaxation Nuclear Magnetic Resonance. *Langmuir* **2017**, *33* (35), 8724−8729.
(60) Cooper, C. L.; Cosgrove, T.; van Duijneveldt, J. S.; Murray, M.; Prescott, S. W. The Use of Solvent Relaxation NMR to Study Colloidal Suspensions. *Soft Matter* **2013**, *9* (30), 7211.
(61) Kwok, D. Y.; Neumann, A. W. Contact Angle Measurement and Contact Angle Interpretation. *Adv. Colloid Interface Sci.* **1999**, *81* (3), 167−249.
(62) Fairhurst, D.; Sharma, R.; Takeda, S.; Cosgrove, T.; Prescott, S. W. Fast NMR Relaxation, Powder Wettability and Hansen Solubility Parameter Analyses Applied to Particle Dispersibility. *Powder Technol.* **2021**, *377*, 545−552.
(63) Brownstein, K. R.; Tarr, C. E. Importance of Classical Diffusion in NMR Studies of Water in Biological Cells. *Phys. Rev. A* **1979**, *19* (6), 2446−2453.
(64) Othmer, D. F.; Thakar, M. S. Correlating Diffusion Coefficient in Liquids. *Ind. Eng. Chem.* **1953**, *45* (3), 589−593.
(65) Moore, J. W.; Wellek, R. M. Diffusion Coefficients of N-Heptane and n-Decane in n-Alkanes and n-Alcohols at Several Temperatures. *J. Chem. Eng. Data* **1974**, *19* (2), 136−140.
(66) Kleinberg, R. L.; Kenyon, W. E.; Mitra, P. P. Mechanism of NMR Relaxation of Fluids in Rock. *J. Magn. Reson., Ser. A* **1994**, *108* (2), 206−214.
(67) Ono, Y.; Shikata, T. Contrary Hydration Behavior of *N*-Isopropylacrylamide to Its Polymer, P(NIPAm), with a Lower Critical Solution Temperature. *J. Phys. Chem. B* **2007**, *111* (7), 1511−1513.

https://doi.org/10.1021/jacsau.3c00384
JACS Au 2023, 3, 2826−2834

(68) Fieremans, E.; De Deene, Y.; Delputte, S.; Özdemir, M. S.; Achten, E.; Lemahieu, I. The Design of Anisotropic Diffusion Phantoms for the Validation of Diffusion Weighted Magnetic Resonance Imaging. *Phys. Med. Biol.* **2008**, *53* (19), 5405−5419.
(69) Jabarin, S. A.; Lofgren, E. A. Effects of Water Absorption on Physical Properties and Degree of Molecular Orientation of Poly (Ethylene Terephthalate). *Polym. Eng. Sci.* **1986**, *26* (9), 620−625.
(70) Hansen, E. W.; Fonnum, G.; Weng, E. Pore Morphology of Porous Polymer Particles Probed by NMR Relaxometry and NMR Cryoporometry. *J. Phys. Chem. B* **2005**, *109* (51), 24295−24303.
(71) Chatzi, E. G.; Koenig, J. L. Morphology and Structure of Kevlar Fibers: A Review. *Polym.−Plast. Technol. Eng.* **1987**, *26* (3−4), 229−270.
(72) Cosimbescu, L.; Malhotra, D.; Pallaka, M. R.; Swita, M. S. Kevlar-like Aramid Polymers from Mixed PET Waste. *ACS Omega* **2022**, *7* (36), 32026−32037.
(73) Jeong, H.-C.; Park, H.-G.; Lee, J. H.; Jang, S. B.; Oh, B.-Y.; Seo, D.-S. Ion Beam-Induced Topographical and Chemical Modification on the Poly(Styrene-Co-Allyl Alcohol) and Its Effect on the Molecular Interaction between the Modified Surface and Liquid Crystals. *Mater. Chem. Phys.* **2016**, *182*, 94−100.
(74) Lee, V. A.; Craig, R. G.; Filisko, F. E.; Zand, R. Preparation and Characterization of High-Surface-Area Polymer Substrates for Microcalorimetry. *J. Biomed. Mater. Res.* **1996**, *31* (1), 51−62.
(75) Fávaro, S.; Rubira, A. F.; Muniz, E. C.; Radovanovic, E. Surface Modification of HDPE, PP, and PET Films with KMnO4/HCl Solutions. *Polym. Degrad. Stab.* **2007**, *92* (7), 1219−1226.
(76) Ellison, A. H.; Zisman, W. A. Wettability Studies on Nylon, Polyethylene Terephthalate and Polystyrene. *J. Phys. Chem. A* **1954**, *58* (6), 503−506.
(77) Wynne, A.; Frisch, J. R.; Britten, C.; Walters, K. B. Synthesis, Characterization, and Stability of Poly(Ethylene-Co-Acrylic Acid) Films Surface Functionalized with Fluorescent Moieties. *React. Funct. Polym.* **2020**, *152*, No. 104598.
(78) Fan, G.; Zhao, J.; Zhang, Y.; Guo, Z. Grafting Modification of Kevlar Fiber Using Horseradish Peroxidase. *Polym. Bull.* **2006**, *56* (4−5), 507−515.
(79) Huang, K.; Yang, X.; Ma, Y.; Sun, G.; Nitin, N. Incorporation of Antimicrobial Bio-Based Carriers onto Poly(Vinyl Alcohol- *Co* -Ethylene) Surface for Enhanced Antimicrobial Activity. *ACS Appl. Mater. Interfaces* **2021**, *13* (30), 36275−36285.
(80) Canal, C.; Molina, R.; Bertran, E.; Erra, P. Wettability, Ageing and Recovery Process of Plasma-Treated Polyamide 6. *J. Adhes. Sci. Technol.* **2004**, *18* (9), 1077−1089.
(81) Tuteja, A.; Choi, W.; Ma, M.; Mabry, J. M.; Mazzella, S. A.; Rutledge, G. C.; McKinley, G. H.; Cohen, R. E. Designing Superoleophobic Surfaces. *Science* **2007**, *318* (5856), 1618−1622.
(82) Blossey, R. Self-Cleaning Surfaces — Virtual Realities. *Nat. Mater.* **2003**, *2* (5), 301−306.
(83) Krzywinski, M.; Altman, N. Multiple Linear Regression. *Nat. Methods* **2015**, *12* (12), 1103−1104.
(84) Borcia, C.; Borcia, G.; Dumitrascu, N. Relating Plasma Surface Modification to Polymer Characteristics. *Appl. Phys. A* **2008**, *90* (3), 507−515.
(85) Junkar, I.; Cvelbar, U.; Vesel, A.; Hauptman, N.; Mozetič, M. The Role of Crystallinity on Polymer Interaction with Oxygen Plasma. *Plasma Processes Polym.* **2009**, *6* (10), 667−675.
(86) Borcia, C.; Punga, I. L.; Borcia, G. Surface Properties and Hydrophobic Recovery of Polymers Treated by Atmospheric-Pressure Plasma. *Appl. Surf. Sci.* **2014**, *317*, 103−110.

https://doi.org/10.1021/jacsau.3c00384
JACS Au 2023, 3, 2826−2834